Proposition of a candidate model for IGRF-13

Baerenzung Julien[1], Sanchez Sabrina[2], Wicht Johannes[2], and Holschneider Matthias[1]

[1]Institute for Mathematics, University of Potsdam
[2]Max Planck Institute for solar system research, Göttingen

October 1, 2019

With the present letter, we would like to candidate for the next IGRF model. We produced an internal field model for the 2020.0 epoch, a DGRF candidate model for the year 2015.0, and a secular variation model for the $2020.0 - 2025.0$ period.
Our model is deriving from the sequential assimilation of CHAMP and Swarm Alpha and Bravo vector field measurements, through a Kalman filter approach.
In the following we describe the data set we are using, the method we are following and the candidate products we are proposing.

1 Data

As previously mentioned, our model is currently uniquely deriving from the vector field measurements of the CHAMP and SWARM low orbiting satellites. For CHAMP, level-2 data were sampled at a rate of 1 datum every 10 seconds under the condition that the vector field magnetometer (VFM) and the star tracker (STR) instruments were functioning in nominal mode. Because very early in the SWARM mission (September 2014), satellite Charlie was subjected to a failure of its absolute scalar magnetometers, only level-1B observations from SWARM Alpha and Bravo are considered for the model derivation. In order for the CHAMP and SWARM data to exhibit a similar rate of occurrence, measurements were taken simultaneously from SWARM Alpha and Bravo every 20 seconds. As for the CHAMP dataset, observations were rejected whenever the STR cameras or the VFM's were not operating in nominal mode .
At low geomagnetic latitudes (between $\pm 60°$) only night time data are kept. This is achieved by eliminating every measurement taken when the satellites are exposed to the sunlight.
Independently of the satellites location, the following additional selection criteria were also applied to the dataset:

- The z-component of the Interplanetary magnetic field(IMF) is positive.
- The geomagnetic activity index $Kp < 2^0$ during the time of observation and $Kp \leq< 2^+$ during the three preceding hours.

No specific weight was a priori applied to any of the data.
All in all the dataset is composed of 2118063 vector field measurements for CHAMP and 2422149 for SWARM for a total of 4540212 measurements. The temporal distribution of the data is shown of figure 1.

2 Model

2.1 Magnetic sources

The different contributions to the observations are described in terms of magnetic sources of either internal or external origin. Except for the source associated with field aligned currents (FACs), each of these contributions b_i is deriving from a potential V_i such as:

$$b_i(r, \theta, \phi, t) = -\nabla V_i(r, \theta, \phi, t) \ . \tag{1}$$

For the magnetic field generated by field aligned currents, we followed the study of [Waters et al., 2001] and express it through the potential V_{fac} as following:

$$b_{fac}(r, \theta, \phi, t) = -r \times \nabla V_{fac}(r, \theta, \phi, t) \ . \tag{2}$$

The potentials are expanded in spherical harmonics for respectively internal and external sources as follows:

$$V_i^i(r, \theta, \phi, t) = a \sum_l \sum_{m=-l}^{m=l} \left(\frac{a_i}{r}\right)^{l+1} g_i^i(l, m, t) Y_{l,m}(\theta, \phi) \tag{3}$$

$$V_i^e(r, \theta, \phi, t) = a \sum_l \sum_{m=-l}^{m=l} \left(\frac{r}{a_i}\right)^{l} g_i^e(l, m, t) Y_{l,m}(\theta, \phi) \tag{4}$$

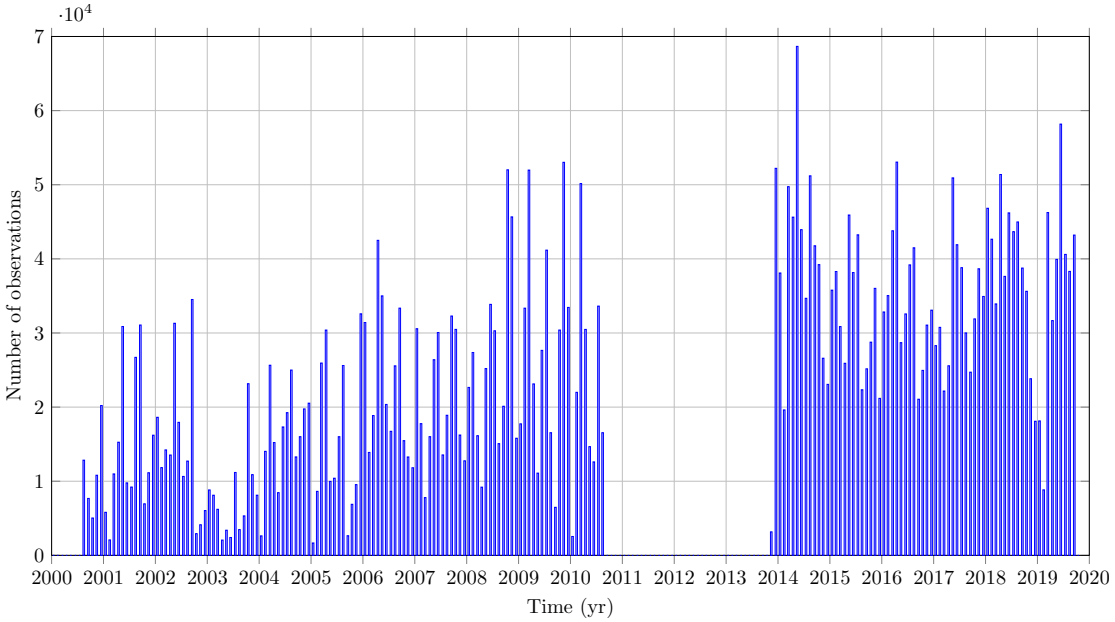

Figure 1: Total number of vector field measurements for bins of 1 month length.

where $Y_{l,m}$ are Schmidt semi-normalized spherical harmonics (SH) of degree l and order m, a_i is a reference radius, and $g_i(l,m,t)$ (later referred as g_i) are the spherical harmonics coefficients expressed at this radius.
The model is composed of 7 magnetic sources as detailed in table 1.

Table 1: Magnetic sources considered in the model. l_{max} corresponds to the maximum degree of the SH expansion, for the three following types of SH decomposition: standard where the SH orders are restricted to $m = [-l, l]$, zonal with $m = 0$ and zonal iso where $m = \{0, 1, -1\}$.

Source	Coordinate system	Source type	l_{max}	SH decompostion
Core field g_c	Geographic	Internal	20	Standard
Lithospheric field g_l	Geographic	Internal	150	Standard
Remote magnetospheric field g_{rm}	Geocentric solar magnetospheric	External	1	Zonal
Close magnetospheric field g_m	Solar magnetic	External	15	Zonal
Fluctuating magnetospheric field g_{fm}	Solar magnetic	External	15	Zonal iso
Residual ionospheric/ induced g_i	Geomagnetic	Internal	50	Zonal iso
Field aligned currents g_{fac}	Solar magnetic	External	15	Zonal iso

2.2 Prior characterization

Following the studies of [Hulot and Le Mouël, 1994, Gillet et al., 2013, Holschneider et al., 2016], each magnetic source g_i is a priori characterized by a full space-time covariance matrix such as:

$$E[g_i(t)g_i(t+\tau)] = \begin{pmatrix} \Sigma^{\infty}_{g_i} & c_i(\tau)\Sigma^{\infty}_{g_i} \\ \Sigma^{\infty}_{g_i} c_i(\tau)^T & \Sigma^{\infty}_{g_i} \end{pmatrix} , \tag{5}$$

where $\Sigma^{\infty}_{g_i}$ corresponds to the stationary state spatial covariance matrix associated with g_i, and $c(\tau)$ is a temporal correlation function depending on the time lag τ. The covariance matrices $\Sigma^{\infty}_{g_i}$ are assumed to derive from imposed energy spectra $E^{\infty}_i(l, a_i)$, expressed at given radii a_i, such as:

$$\begin{aligned} \Sigma^{\infty}_{g_i}(l,m,l',m',r=a_i) &= E[g_i(l,m)g_i(l',m')] \\ &= \frac{E^{\infty}_i(l,a_i)}{N_m \times Fs(l)}\delta(l-l')\delta(m-m') \end{aligned} \tag{6}$$

where N_m is the number of modeled spherical harmonics coefficients per degree l, and Fs is the pre-factor of the energy spectra given by $Fs(l) = l+1$ and $Fs(l) = l$ for respectively internal and external sources. Two types of spectra are used for the model, flat ones, with $E^{\infty}_i(l) = A^2_i$ where A_i is a magnitude, and spectra of the form $E^{\infty}_i(l) = A^2_i(2l+1)Fs(l)$, making equation 6 equivalent to the correlation kernels proposed by [Holschneider et al., 2016].
Temporal constraints are prescribed by the type of correlation functions introduced by [Gillet et al., 2013, Gillet et al., 2015] in the context of geomagnetic modeling. The latter are deriving from auto-regressive processes, and read for respectively

first and second order processes:

$$c_i(\tau) = \exp\left[-|\tau|/\tau_i(l)\right] \quad (7)$$

$$c_i(\tau) = (1 + (|\tau|/\tau_i(l)))\exp\left[-(|\tau|/\tau_i(l))\right] \quad , \quad (8)$$

where $\tau_i(l)$ are scale dependent characteristic timescales. The latter are parameterized with power laws such as:

$$\tau_i(l) = M_i^2 l^{-\alpha_i} \quad (9)$$

with M_i some magnitudes and α_i some slopes. Together with the spectra amplitudes A_i and the radii a_i, M_i and α_i are the parameters of the spatio temporal correlation functions used to a priori constrain the different magnetic sources. These parameters are directly estimated with a subsample of the dataset following a procedure which is not detail here. However, the stationary state energy spectra of the different sources given on table 1, are shown at the Earth's surface on figure 2. As a comparison for the internal sources, the energy spectra of the CHAOS-6 core field model of [Finlay et al., 2016] in 2015.0 and the LCS-1 lithopsheric field model of [Olsen et al., 2017] are respectively displayed with black and red circles. The different timescales τ_i are exhibiting values ranging from the minute for the magnetic field induced by FAC to several hundreds of years for the large scale part of the core field. The lithospheric field is a priori assumed to be static.

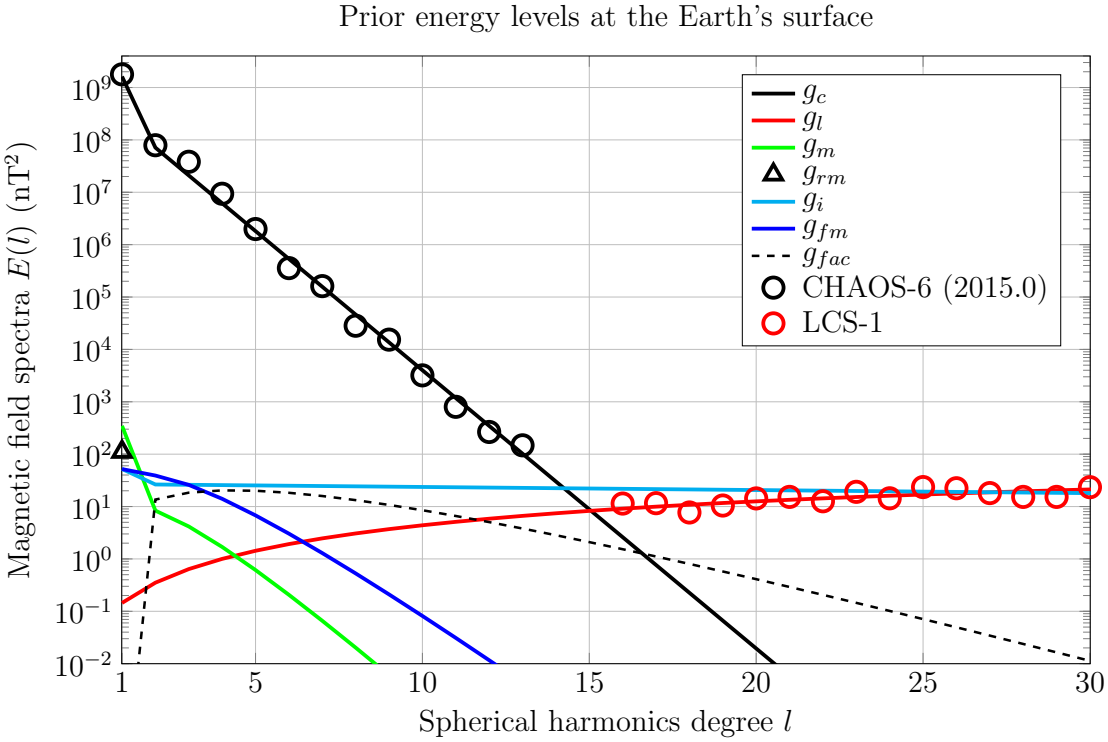

Figure 2: Stationary state energy spectra at the Earth's surface of the different magnetic sources given in table 1. Black and red circles are the energy spectra of respectively the CHAOS-6 core field model of [Finlay et al., 2016] in 2015.0 and the LCS-1 lithopsheric field model of [Olsen et al., 2017].

2.3 Sequentialization

Instead of performing a full Bayesian inversion with the covariance matrices given by equation 5 as a prior information, the inverse problem is sequentialized through a Kalman filter approach [Kalman, 1960]. To do so, dynamical equations are required to forecast the statistical properties of the different modeled sources. As previously mentioned, the correlation functions we wish to a priori impose are deriving form autoregressive processes. In their continuous form the latter are given for respectively first and second orders by:

$$\partial_t g_i(l,m,t) + \frac{1}{\tau_i(l)} g_i(l,m,t) = \sigma_i(l)\dot{\omega}(t) \quad (10)$$

$$\partial_t^2 g_i(l,m,t) + \frac{2}{\tau_i(l)}\partial_t g_i(l,m,t) + \frac{1}{\tau^2(l)} g_i(l,m,t) = \sigma_i(l)\dot{\omega}(t) \quad (11)$$

where $\dot{\omega}(t)$ is a Gaussian withe noise scaled by the factor $\sigma_i(l)$. These equations have analytical solutions which can be written under the general form:

$$z_i(t+\tau) = F_i(\tau) z_i(t) + \xi_i(t) \quad (12)$$

where the Gaussian white noise ξ_i is randomly drawn from the distribution $\mathcal{N}\left(0, \Sigma^{\infty}_{z_i} - F_i \Sigma^{\infty}_{z_i} F_i^T\right)$.
For magnetic sources characterized by first auto regressive processes, $z_i = g_i$ and F_i is given by:

$$F_i(l,\tau) = \exp\left[-|\tau|/\tau_i(l)\right]. \tag{13}$$

The core field evolution is prescribed by a second order auto regressive process, therefore in this case, $z_i = (g_i, \partial_t g_i)^T$ and:

$$F_i(l,\tau) = \begin{pmatrix} 1+|\tau|/\tau_i(l) & \tau/\tau_i(l) \\ -\tau/\tau_i^2(l) & 1-|\tau|/\tau_i(l) \end{pmatrix} \exp\left[-|\tau|/\tau_i(l)\right] \tag{14}$$

2.4 Sequential assimilation

The model consists in a vector $\mathbf{z}$ containing the spherical harmonics coefficients of every magnetic sources (including the SH expansion of the secular variation). Its evaluation is performed with a Kalman filter algorithm which proceeds sequentially in two steps. In the first step, referred as the forecast, the evolution of the mean model $E[\mathbf{z}]$ together with its associated covariance matrix $\mathbf{\Sigma_z}$ are predicted until observation time. In the second step, namely the analysis, the model is corrected accordingly to the data through a Bayesian inversion.
To predict the simultaneous evolution of the different magnetic sources with the auto-regressive processes presented in the previous section, a matrix $\mathbf{F}$ containing all the matrices F_i, and a matrix $\tilde{\mathbf{\Sigma}} = \mathbf{\Sigma}^{\infty} - \mathbf{F}\mathbf{\Sigma}^{\infty}\mathbf{F}^T$ characterizing the white noise of the complete evolution model, are constructed. Therefore, at a step $k-1$ the model is forecasted accordingly to the following relation:

$$E[\mathbf{z}_{k|k-1}] = \mathbf{F}_{k-1} E[\mathbf{z}_{k-1}] \tag{15}$$

$$\mathbf{\Sigma}_{\mathbf{z}_{k|k-1}} = \mathbf{F}_{k-1} \mathbf{\Sigma}_{\mathbf{z}_{k-1}} \mathbf{F}_{k-1}^T + \tilde{\mathbf{\Sigma}}\ . \tag{16}$$

If at iteration k some measurements are available, the model is then corrected with the formulations:

$$\mathbf{K}_k = \mathbf{\Sigma}_{\mathbf{z}_{k|k-1}} \mathbf{H}_k^T \left(\mathbf{H}_k \mathbf{\Sigma}_{\mathbf{z}_{k|k-1}} \mathbf{H}_k^T\right) \tag{17}$$

$$E[\mathbf{z}_{k|\mathbf{d}_k}] = E[\mathbf{z}_{k|k-1}] + \mathbf{K}_k \left(d_k - \mathbf{H}_k E[\mathbf{z}_{k|k-1}]\right) \tag{18}$$

$$\mathbf{\Sigma}_{\mathbf{z}_{k|\mathbf{d}_k}} = \left(\mathbf{I} - \mathbf{K}_k \mathbf{H}_k\right) \mathbf{\Sigma}_{\mathbf{z}_{k|k-1}} \tag{19}$$

where $\mathbf{K}_k$ is the Kalman gain matrix and $\mathbf{H}_k$ is the operator projecting the model to the data d_k at iteration k. $\mathbf{d}_k$ corresponds to the entire dataset until step k. Note that the time step of the algorithm has been set to $\tau = 1$ hour.

2.5 Smoothing

With the Kalman filter algorithm, one gets access to the distribution $p(\mathbf{z}_k|\mathbf{d}_k)$. To obtain $p(\mathbf{z}_k|\mathbf{d})$ the posterior distribution of the model at iteration k given the entire dataset $\mathbf{d}$, one can apply a smoothing algorithm. In this study we chose the formulation of [Rauch et al., 1965]. Starting at the last iteration of the Kalman filter algorithm, the smoothing algorithm performs iteratively backward in time accordingly to the following step:

$$\mathbf{G}_k = \mathbf{\Sigma}_{\mathbf{z}_{k|\mathbf{d}_k}} \mathbf{F}_k^T \mathbf{\Sigma}_{\mathbf{z}_{k+1|k}} \tag{20}$$

$$E[\mathbf{z}_{k|\mathbf{d}}] = E[\mathbf{z}_{k|\mathbf{d}_k}] + \mathbf{G}_k \left(E[\mathbf{z}_{k+1|\mathbf{d}}] - E[\mathbf{z}_{k+1|k}]\right) \tag{21}$$

$$\mathbf{\Sigma}_{\mathbf{z}_{k|\mathbf{d}}} = \mathbf{\Sigma}_{\mathbf{z}_{k|\mathbf{d}_k}} + \mathbf{G}_k \left(\mathbf{\Sigma}_{\mathbf{z}_{k+1|\mathbf{d}}} - \mathbf{\Sigma}_{\mathbf{z}_{k+1|k}}\right) \mathbf{G}_k^T\ . \tag{22}$$

3 Candidate products

The models that we propose as candidates for IGRF-13 in 2020.0 directly derives from the Kalman filter solution at the last epoch of data occurrence in 2019.74 (September the 26^{th}). This solution is forwarded in time until 2020.0 with the forecast step of the Kalman filter algorithm as following:

$$E[\mathbf{z}](t=2020.0) = \mathbf{F}_{\tau=0.26yr} E[\mathbf{z}](t=2019.74) \tag{23}$$

$$\mathbf{\Sigma_z}(t=2020.0) = \mathbf{F}_{\tau=0.26yr} \mathbf{\Sigma_z}(t=2019.74) \mathbf{F}^T_{\tau=0.26yr} + \tilde{\mathbf{\Sigma}}_{\tau=0.26yr}\ . \tag{24}$$

Our secular variation is therefore the mean secular variation estimation in 2020.0, namely $E[\partial_t g_c](t=2020.0)$. The associated uncertainties are obtained by taking the square root of the diagonal elements of the covariance matrix $\Sigma_{\partial_t g_c}(t=2020)$ providing the standard deviation corresponding to each SH coefficients of $\partial_t g_c$. The file containing the secular variation and its uncertainties is named **SV_2020.dat**.

Our internal field model in 2020.0 is the sum of the mean core field and the mean lithospheric field at this epoch $(E[g_c] + E[g_l])$. The uncertainties estimate is deriving from the covariance matrix $\Sigma_{g_c+g_l} = \Sigma_{g_c} + \Sigma_{g_l} + \Sigma_{g_{cl}} + \Sigma^T_{g_{cl}}$ in 2020.0, where $\Sigma_{g_{cl}}$ is the cross covariance between the core field and the lithospheric field. The square root of each diagonal elements of $\Sigma_{g_c+g_l}$ provides the standard deviation associated with $(E[g_c] + E[g_l])$. The model is called **MF_2020.dat**.

Our candidate for the DGRF 2015.0 model is constructed in a similar manner as our 2020.0 internal field model, except that the core and the lithospheric fields are taken from the smoothing solution. This model is named **MF_2015.dat**.

References

[Finlay et al., 2016] Finlay, C. C., Olsen, N., Kotsiaros, S., Gillet, N., and Tøffner-Clausen, L. (2016). Recent geomagnetic secular variation from Swarm and ground observatories as estimated in the CHAOS-6 geomagnetic field model. *Earth, Planets, and Space*, 68:112.

[Gillet et al., 2015] Gillet, N., Jault, D., and Finlay, C. C. (2015). Planetary gyre, time-dependent eddies, torsional waves, and equatorial jets at the Earth's core surface. *Journal of Geophysical Research (Solid Earth)*, 120:3991–4013.

[Gillet et al., 2013] Gillet, N., Jault, D., Finlay, C. C., and Olsen, N. (2013). Stochastic modeling of the Earth's magnetic field: Inversion for covariances over the observatory era. *Geochemistry, Geophysics, Geosystems*, 14:766–786.

[Holschneider et al., 2016] Holschneider, M., Lesur, V., Mauerberger, S., and Baerenzung, J. (2016). Correlation-based modeling and separation of geomagnetic field components. *Journal of Geophysical Research (Solid Earth)*, 121:3142–3160.

[Hulot and Le Mouël, 1994] Hulot, G. and Le Mouël, J. L. (1994). A statistical approach to the Earth's main magnetic field. *Physics of the Earth and Planetary Interiors*, 82(3-4):167–183.

[Kalman, 1960] Kalman, R. E. (1960). A New Approach to Linear Filtering and Prediction Problems. *Journal of Basic Engineering*, 82:35–45.

[Olsen et al., 2017] Olsen, N., Ravat, D., Finlay, C. C., and Kother, L. K. (2017). LCS-1: a high-resolution global model of the lithospheric magnetic field derived from CHAMP and Swarm satellite observations. *Geophysical Journal International*, 211(3):1461–1477.

[Rauch et al., 1965] Rauch, H. E., Striebel, C. T., and Tung, F. (1965). Maximum likelihood estimates of linear dynamic systems. *AIAA Journal*, 3(8):1445–1450.

[Waters et al., 2001] Waters, C. L., Anderson, B. J., and Liou, K. (2001). Estimation of global field aligned currents using the iridium® System magnetometer data. *Geophysical Research Letters*, 28(11):2165–2168.